Cellular palmitoylation and trafficking of lipidated peptides

Jeremiah M. Draper,[*] Zuping Xia,[†] and Charles D. Smith[1,*,†]

Department of Pharmacology,[*] Pennsylvania State University College of Medicine, Hershey, PA; and Department of Pharmaceutical Sciences,[†] Medical University of South Carolina, Charleston, SC

Abstract **Many important signaling proteins require the posttranslational addition of fatty acid chains for their proper subcellular localization and function. One such modification is the addition of palmitoyl moieties by enzymes known as palmitoyl acyltransferases (PATs). Substrates for PATs include C-terminally farnesylated proteins, such as H- and N-Ras, as well as N-terminally myristoylated proteins, such as many Src-related tyrosine kinases. The molecular and biochemical characterization of PATs has been hindered by difficulties in developing effective methods for the analysis of PAT activity. In this study, we describe the use of cell-permeable, fluorescently labeled lipidated peptides that mimic the PAT recognition domains of farnesylated and myristoylated proteins. These PAT substrate mimetics are accumulated by SKOV3 cells in a saturable and time-dependent manner. Although both peptides are rapidly palmitoylated, the SKOV3 cells have a greater capacity to palmitoylate the myristoylated peptide than the farnesylated peptide. Confocal microscopy indicated that the palmitoylated peptides colocalized with Golgi and plasma membrane markers, whereas the corresponding nonpalmitoylatable peptides accumulated in the Golgi but did not traffic to the plasma membrane. Overall, these studies indicate that the lipidated peptides provide useful cellular probes for quantitative and compartmentalization studies of protein palmitoylation in intact cells.**—Draper, J. M., Z. Xia, and C. D. Smith. **Cellular palmitoylation and trafficking of lipidated peptides.** ***J. Lipid Res.*** **2007.** 48: **1873–1884.**

Supplementary key words palmitoyl acyltransferase • Ras • lipidation • subcellular trafficking

A major mechanism by which cells regulate the subcellular localization of proteins is through posttranslational lipid modifications that increase the hydrophobicity of proteins, promote their localization to specific cellular compartments, and/or alter their conformation (reviewed in Refs. 1–6). Many important signaling proteins, including Ras proteins and Src-related tyrosine kinases, require localization to the plasma membrane to activate their downstream effector proteins (2, 7–12). Accumulating evidence demonstrates that targeting of these signaling proteins to the plasma membrane is facilitated by posttranslational lipidation reactions and that blocking the enzymes that catalyze these reactions is an effective means of blocking signaling through these pathways (13–17).

One such lipidation process is thioesterification, also known as palmitoylation, in which a 16 carbon palmitate group is covalently attached to one or more cysteine residues in a target protein. A variety of proteins are known to be palmitoylated (3, 7, 18), and many of these proteins can be separated into groups based on motifs adjacent to the site(s) of palmitoylation (3). One group of palmitoylated proteins contains a C-terminal farnesyl motif, whereas a second group contains an N-terminal myristoyl motif. Both types of proteins undergo multistep posttranslational modification to effectively localize to the plasma membrane. The farnesylated group, which includes proteins such as H-, N-, and K2A-Ras (3, 18), contains a C-terminal CAAX motif that is required for palmitoylation of a cysteine located near the C-terminal farnesylcysteine (19). After farnesylation of the cysteine of the CAAX motif by farnesyltransferase, the AAX residues are proteolytically removed and the new C terminus is carboxymethylated. The final modification consists of the attachment of palmitate groups to cysteines near the C-terminal farnesylcysteine through a thioester linkage to the sulfhydryl of the target cysteine, which is catalyzed by a palmitoyl acyltransferase (PAT) enzyme (13, 19). This final lipid modification is required to target these Ras isoforms to the membrane and for complete activation of their transforming ability (13, 20, 21). The myristoylated and palmitoylated group of proteins includes several Src-related kinases such as Lck and Fyn and is characterized by an N-terminal methionylglycyl sequence closely followed by a cysteine residue. In this case, the processing involves the cleavage of the

Manuscript received 1 September 2006 and in revised form 12 April 2007 and in re-revised form 18 May 2007.

Published, JLR Papers in Press, May 24, 2007.
DOI 10.1194/jlr.M700179-JLR200

Abbreviations: AUC, area under the curve; LDH, lactate dehydrogenase; NBD, 7-nitro-2-1,3-benzoxadiazol-4-yl; PAT, palmitoyl acyltransferase; WGA, wheat germ agglutinin.

[1] To whom correspondence should be addressed.
e-mail: smithchd@musc.edu

N-terminal methionine, thereby creating an N-terminal glycine that is modified by the addition of a myristate moiety through the action of *N*-myristoyltransferase. Similar to the reactions discussed above, the myristoylation modification is necessary for the subsequent palmitoylation of one or more cysteine residues near the N-terminus of the protein via a PAT (3, 22, 23). As with the C-terminal modified proteins, the palmitoylation modification is required for effective localization of these proteins to the plasma membrane and for effective signal transduction (14–16).

Because distinct motifs at the C and N termini of these proteins direct their palmitoylation, we (24–27) and others (3) have hypothesized that different PAT enzymes recognize and palmitoylate these classes of proteins. The existence of motif-specific PATs is of interest because of the roles of palmitoylated proteins in the cell. Many of these proteins, such as the Ras proteins and Src-related tyrosine kinases, are involved in signaling pathways that drive cellular survival and proliferation (28–31). The fact that the functions of these proteins are predicated on their specified subcellular localizations makes the enzymes that catalyze their posttranslational modifications attractive drug targets. In fact, the enzymes involved in the posttranslational modifications of Ras proteins are considered prime targets for anticancer drugs (32, 33). However, the primary focus for the development of anti-Ras agents has been on the process of farnesylation. This is partly because the farnesyltransferases have been cloned (34, 35) and used in screens to identify and develop inhibitors (36, 37). In contrast, the identification and characterization of human PATs has been hindered by the lack of defined assays to characterize these enzymes and to identify small molecule inhibitors.

We previously described indirect cellular assays that can be used to screen chemical libraries for PAT inhibitors (27) and in vitro PAT assays that can be used for low-throughput confirmation of PAT inhibitory activity (24, 25). However, these methods are still insufficient to directly measure PAT activity in intact cells, which would be highly useful in the molecular identification of human PAT enzymes and biochemical studies of the regulation of these PATs. Therefore, in these studies, we sought to develop quantitative and efficient cellular assays to characterize PAT activity in intact cells using peptides that mimic the palmitoylation motifs of farnesyl- and myristoyl-directed PATs. The data demonstrate that synthetic lipidated peptides provide excellent tools to conduct such studies on PAT activity as well as studies of the role of palmitoylation in the subcellular trafficking of lipidated proteins.

MATERIALS AND METHODS

Materials

Palmitoyl-CoA, 2-mercaptoethanol, and DMSO were purchased from Sigma (St. Louis, MO). Alexa Flour 594-conjugated wheat germ agglutinin (WGA; W11262), Hoechst 33342, and BODIPY TR C_5-ceramide (B34400) were purchased from Molecular Probes (Eugene, OR). The fluorescent peptides 7-nitro-2-1,3-benzoxadiazol-4-yl (NBD)-CLC(OMe)-Farn and Myr-GC-NBD were synthesized as *t*-butyl-disulfide-protected precursors by solution-phase chemistry using mild conditions to maintain chemically labile functional groups (e.g., the farnesyl-cysteine thioether linkage), as described previously (38, 39). These peptides (1 or 5 mM in DMSO) were stored under argon at −80°C and deprotected immediately before use by incubation with 2-mercaptoethanol/DMSO (2.7:97.3 or 12:88, v/v, respectively) containing 50 mM Tris, pH 8.0, at 55°C for 20 min with agitation. Peptides containing alanine residues in the place of the cysteine residues [i.e., NBD-ALC(OMe)-Farn and Myr-GA-NBD], to be used as nonpalmitoylatable controls, were synthesized by parallel methods.

Cell culture

All cell culture reagents were obtained from Gibco Co. (Grand Island, NY). SKOV3 cells (American Type Culture Collection HTB-77) were maintained in DMEM containing 10% fetal bovine serum, 1 mM sodium pyruvate, and 50 μg/ml gentamycin at 37°C in an atmosphere of 5% CO_2 and 95% air.

Cytotoxicity assays

To determine the potential cytotoxic effects of the peptides, SKOV3 cells were plated onto 96-well microtiter plates and allowed to attach for 24 h. The peptides were resuspended in DMSO as a vehicle and diluted in standard culture medium to various concentrations. The cells were subsequently incubated with the peptides for 2 h at 37°C. Toxicity was determined by measuring the amount of lactate dehydrogenase (LDH) released, as an indication of cell permeability, using the CytoTox-One Homogeneous Membrane Integrity Assay kit from Promega (Madison, WI).

Cellular palmitoylation assay

In dose-response studies, SKOV3 cells were grown to confluence and incubated for 60 min at 37°C with one of the test peptides (or DMSO as vehicle) in culture medium at final concentrations varying from 0.1 to 80 μM. In time-course studies, the cells were grown to confluence and incubated with one of the test peptides at 1 μM in culture medium at 37°C for times varying from 5 to 120 min. For all experiments, the parent peptides and the palmitoylated peptide products were collected from the cells using the following standard extraction protocol. After incubation with the peptide, the cells were washed twice with ice-cold PBS, killed by the addition of ice-cold 50% methanol, scraped, and transferred to a glass test tube. The peptides were extracted into the organic phase by the addition of potassium carbonate-buffered dichloromethane-water-methanol (4:3:1, v/v) and low-speed centrifugation. The organic phase was transferred to another tube, and the remaining aqueous phase was extracted once more with buffered dichloromethane. The organic fractions were combined, dried under nitrogen, and analyzed immediately by HPLC as indicated below. As controls for the retention times of the nonpalmitoylated and palmitoylated peptides, each peptide (10 μM) was incubated with 100 μM palmitoyl-CoA in high-pH acylation buffer [50 mM citrate, 50 mM phosphate, 50 mM Tris, and 50 mM 3-(cyclohexylamino) propane-1-sulfonic acid, pH 8.2] at 37°C for 10 min with agitation. The samples were extracted as described above and subjected to HPLC analysis as indicated below.

HPLC method for quantifying peptide palmitoylation

Assay extracts were dissolved in 27 μl of DMSO, and the peptides were resolved on a reverse-phase Chromolith RP-8e column

(2 μm, 300 Å, 4.6 mm × 100 mm) using a methanol gradient at a flow rate of 1 ml/min. Initially, the mobile phase was maintained at 30% methanol and 70% water for 1 min, followed by a linear gradient of 30–100% methanol over 5 min. The mobile phase was maintained at 100% methanol for 6 min and then decreased on a linear gradient to 30% methanol over 2 min. The peptides were detected by the fluorescence of their fluorophore NBD at its optimal excitation and emission wavelengths of 465 and 531 nm, respectively. Peptides that eluted at the retention time of peak B (see Fig. 3 below) were shown by mass spectroscopy to be palmitoylated, whereas peptides eluting at any other time were nonpalmitoylated. The mean values of the area under the curve (AUC) for each treatment were converted to femtomoles of peptide using a standard curve generated by direct injection of known quantities of the peptides. The percentage of peptide palmitoylated was calculated as the mass of peak B divided by the total peptide mass in the sample.

Confocal laser microscopy

Confocal microscopy was performed using a Zeiss LSM 510 NLO Laser Scanning Microscope with Multiphoton Excitation and Zeiss software (Confocal Microscopy Core at the Medical University of South Carolina). To monitor the trafficking of the peptides in SKOV3 cells over time, the cells were incubated with Hoechst 33342 (2 μg/ml) for 10 min at 37°C in DMEM without phenol red or serum, washed twice with warm medium, and then incubated with peptide (1 μM). The cells were maintained at 37°C in 5% CO_2, and images were captured at times from 15 to 120 min. To compare the localization of the peptides with the plasma membrane, the cells were incubated with peptide (1 μM) in DMEM without phenol red or serum at 37°C. After 15 min, AF594-WGA (15 μg/ml) was added, and the cells were further incubated for an additional 15 min at 37°C. The medium was then removed, and the cells were washed twice with fresh medium and observed directly by confocal microscopy. Localization of the peptides to the Golgi apparatus was determined by incubating the cells with BODIPY TR C_5-ceramide (0.17 mg/ml) on ice for 30 min (40). The cells were then washed twice with ice-cold HBSS (Gibco), and warm medium containing 1 μM peptide was added. The cells were incubated for 30 min at 37°C, washed twice, and visualized as above. All images presented are single sections.

RESULTS

Cytotoxicity of lipidated peptides

The NBD-CLC(OMe)-Farn peptide (**Fig. 1**) is a farnesylated tripeptide that mimics the C terminus of H-Ras and provides the putative recognition motif for PATs, which palmitoylate the cysteine residue of C-terminally lipidated proteins. The NBD-ALC(OMe)-Farn peptide is identical to NBD-CLC(OMe)-Farn except that it has a nonpalmitoylatable alanine substituted for the cysteine residue. Similarly, the Myr-GC-NBD peptide (Fig. 1) is a myristoylated dipeptide that mimics the N termini of several Src-related tyrosine kinases and provides the putative recognition motif for PATs, which palmitoylate the adjacent cysteine residue. The corresponding nonpalmitoylatable peptide Myr-GA-NBD has an alanine substituted for the cysteine residue. Because of the hydrophobicity of the lipidated peptides, it was necessary to determine their toxicities toward SKOV3 cells under conditions that were used in subsequent experiments. Therefore, the toxicities of the peptides after 2 h were measured using the LDH release assay. As indicated in **Fig. 2A**, there was no induc-

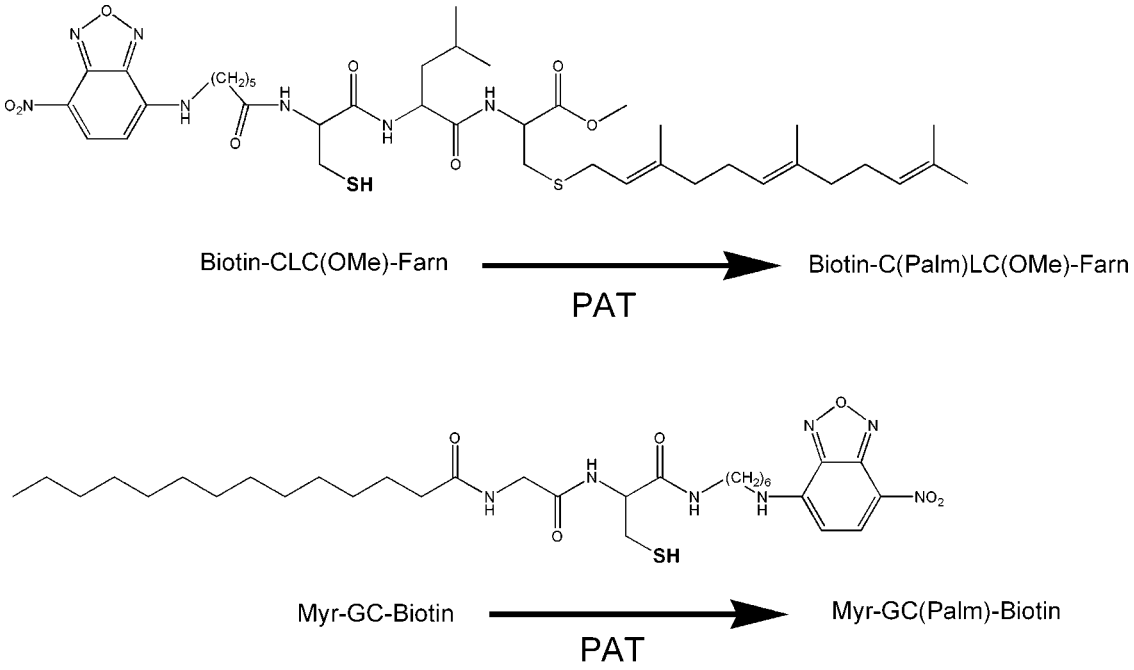

Fig. 1. Structures of lipidated peptides. The 7-nitro-2-1,3-benzoxadiazol-4-yl (NBD)-CLC(OMe)-Farn peptide is a farnesylated tripeptide that mimics the C-terminal recognition motif of farnesylated and palmitoylated proteins such as H-Ras and paralemmin. The Myr-GC-NBD peptide is a myristoylated dipeptide that mimics the N-terminal recognition motif of myristoylated and palmitoylated proteins such as the Src-related tyrosine kinases. PAT, palmitoyl acyltransferase.

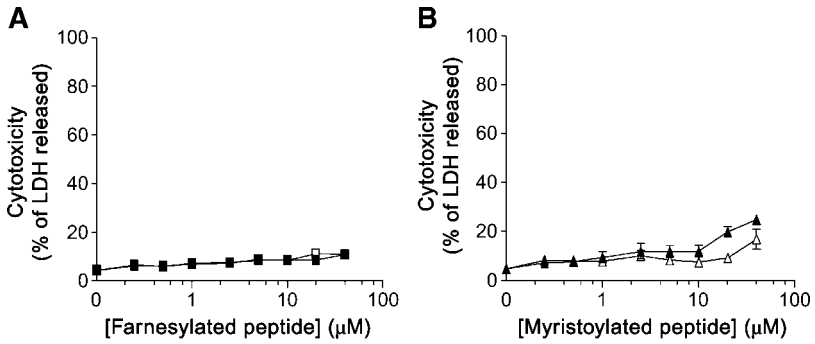

Fig. 2. Cytotoxicity of lipidated peptides. SKOV3 cells were exposed to the indicated concentrations of either NBD-CLC(OMe)-Farn (closed squares) or NBD-ALC(OMe)-Farn (open squares) in A and either Myr-GC-NBD (closed triangles) or Myr-GA-NBD (open triangles) in B for 2 h. The release of lactate dehydrogenase (LDH) into the medium was then measured as an indication of toxicity of the peptides, as described in Materials and Methods.

tion of LDH release from cells treated for 2 h with either the NBD-CLC(OMe)-Farn or the NBD-ALC(OMe)-Farn peptide. In addition, treatment with the Myr-GC-NBD and Myr-GA-NBD peptides caused only a small increase in LDH release at high peptide concentrations (Fig. 2B).

Cellular palmitoylation of lipidated peptides

The elution times of parent and palmitoylated peptides were determined using reverse-phase HPLC analyses. Pure parental (nonpalmitoylated) peptide eluted at the positions defined in the top row of **Fig. 3**. In vitro incubation of the

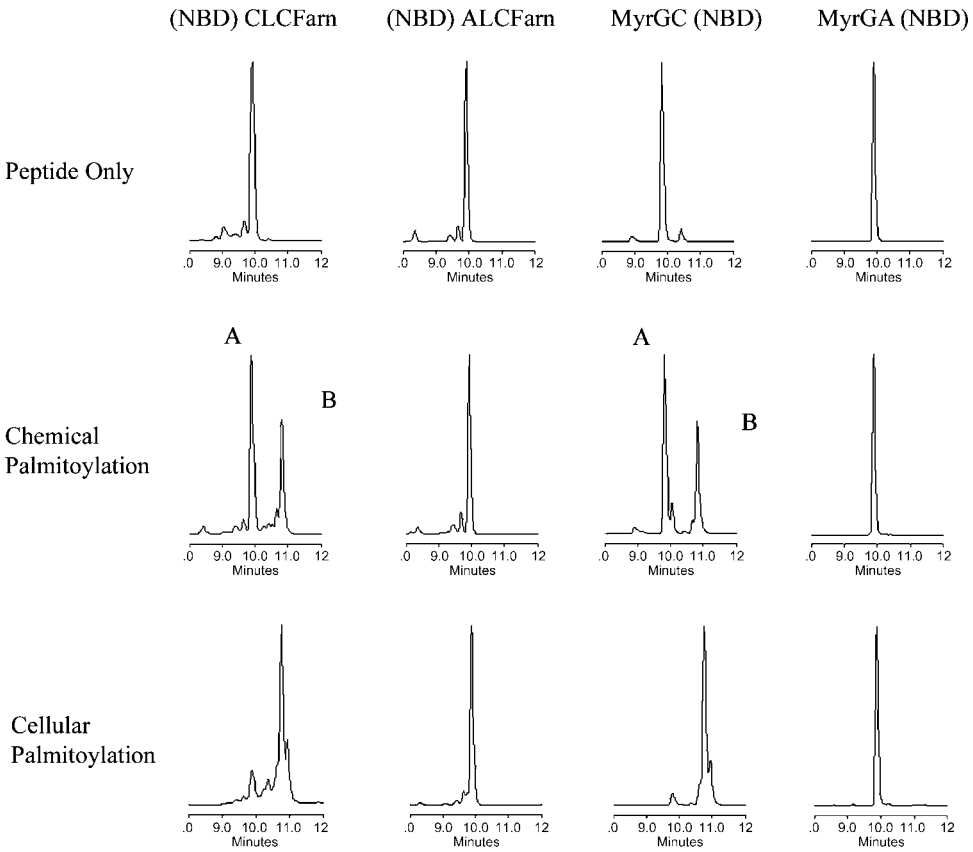

Fig. 3. Chromatograms of NBD-CLC(OMe)-Farn, NBD-ALC(OMe)-Farn, Myr-GC-NBD, and Myr-GA-NBD under multiple conditions. For peptide only, pure peptide was treated with 2-mercaptoethanol and extracted and resolved by HPLC as described in Materials and Methods. For chemical palmitoylation, pure peptide was treated with 2-mercaptoethanol, incubated in vitro with palmitoyl-CoA to induce chemical palmitoylation, and extracted and resolved as above. The nonpalmitoylated substrate peptides elute at the position of peak A, whereas the palmitoylated product peptides elute at the position of peak B. For cellular palmitoylation, peptide was treated with 2-mercaptoethanol, incubated at 1 μM peptide with SKOV3 cells at 37°C for 1 h, and extracted and resolved as stated above.

peptides with palmitoyl-CoA at pH 8.2 allows nonenzymatic palmitoylation. This treatment resulted in the conversion of peak A to peak B (middle row of Fig. 3), which were confirmed by mass spectroscopy to be the palmitoylated forms of the peptides. As expected, replacement of the cysteines with alanines in the NBD-ALC(OMe)-Farn and Myr-GA-NBD peptides blocked their abilities to be palmitoylated. In addition, because the retention times of the nonpalmitoylated and palmitoylated cysteine-containing peptides are well resolved, the method allows for the quantification of the amount of palmitoylated and nonpalmitoylated peptide. Therefore, in further experiments, the AUC of the peak at a retention time equivalent to that of peak B was considered to represent the palmitoylated peptide, and the AUC of peak A was considered to represent the nonpalmitoylated peptide.

Determination of the ability of the peptides to be palmitoylated by intact cells was examined by incubating SKOV3 cells for 60 min at 37°C with a 1 μM concentration of each peptide. The cells were subsequently washed, and the cellular lysates were extracted and subjected to reverse-phase HPLC analysis (bottom row of Fig. 3). The results indicate that the NBD-CLC(OMe)-Farn and Myr-GC-NBD peptides are palmitoylated by SKOV3 cells, manifested as a decrease in peak A and a corresponding increase in peak B. In contrast, the NBD-ALC(OMe)-Farn and Myr-GA-NBD peptides remain nonpalmitoylated, which allows them to be used as nonpalmitoylatable peptides in the cellular localization studies described below.

Kinetics of peptide palmitoylation by SKOV3 cells

To examine the kinetics of peptide palmitoylation in SKOV3 cells, dose-response curves were generated by incubating the cells for 60 min at 37°C with peptides at concentrations of 1–80 μM. As demonstrated in **Fig. 4A**, the cellular uptake of the NBD-CLC(OMe)-Farn peptide increased in a linear manner until the peptide concentration reached 20 μM, whereas the cellular uptake of the Myr-GC-NBD peptide increased in a roughly linear manner until a concentration of 40 μM was reached. At concentrations of 2.5 μM and lower, the uptake of the two peptides was not significantly different; however, at concentrations of 10 μM and greater, the uptake of the Myr-GC-NBD peptide was significantly greater than that of the NBD-CLC(OMe)-Farn peptide.

Figure 4B indicates that significant amounts of nonpalmitoylated NBD-CLC(OMe)-Farn accumulate in cells treated with peptide concentrations of 2.5 μM or greater. In contrast, nearly all of the Myr-GC-NBD peptide is palmitoylated, even when it is given at high concentrations (Fig. 4C). This is summarized in Fig. 4D, which demonstrates that the majority of Myr-GC-NBD peptide is palmitoylated regardless of peptide concentration, whereas maximal palmitoylation of the NBD-CLC(OMe)-Farn peptide occurred at peptide concentrations up to 1.0 μM and decreased significantly at higher concentrations. Because maximal palmitoylation was observed for both peptides at a concentration of 1 μM, this concentration was chosen for all further experiments.

To determine the effects of exposure duration on peptide uptake and palmitoylation, SKOV3 cells were incubated with a 1 μM concentration of either the NBD-CLC(OMe)-Farn or the Myr-GC-NBD peptide at 37°C for times of 5–120 min. As indicated in **Fig. 5A**, both peptides were accumulated by the cells in a linear manner until ~30 min, when uptake of the peptides reached a plateau. The Myr-GC-NBD peptide was rapidly palmitoylated by the cells such that >60% of the peptide was modified at the earliest measurable time point, and levels of nonpalmitoylated peptide did not increase over the 60 min time course. In contrast,

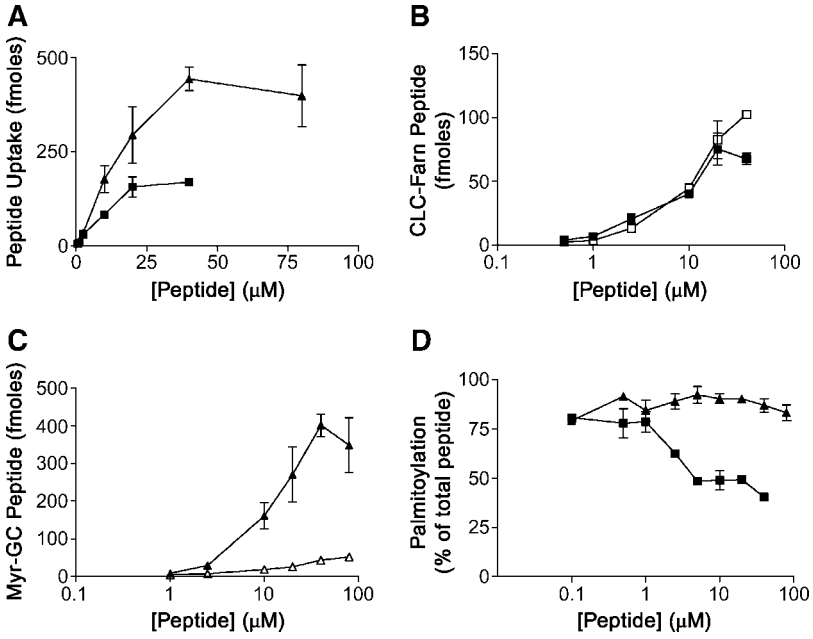

Fig. 4. Dose-response curves for lipidated peptide uptake and palmitoylation by SKOV3 cells. SKOV3 cells were incubated for 60 min at 37°C with the indicated concentrations of NBD-CLC(OMe)-Farn or Myr-GC-NBD peptide. Samples were then extracted and analyzed as described in Materials and Methods. A: The total amount of NBD-CLC(OMe)-Farn (closed squares) or Myr-GC-NBD (closed triangles) peptide accumulation in the cells was determined as the total fluorescence in the samples. B: The amounts of nonpalmitoylated NBD-CLC(OMe)-Farn (open squares) and palmitoylated NBD-CLC(OMe)-Farn (closed squares) are shown. C: The amounts of nonpalmitoylated Myr-GC-NBD (open triangles) and palmitoylated Myr-GC-NBD (closed triangles) are shown. D: The percentages of palmitoylated NBD-CLC(OMe)-Farn (closed squares) and Myr-GC-NBD (closed triangles) peptide are shown. For A–C, values represent means ± SD for triplicate samples in a typical experiment; for D, values represent means ± SEM for three to nine experiments.

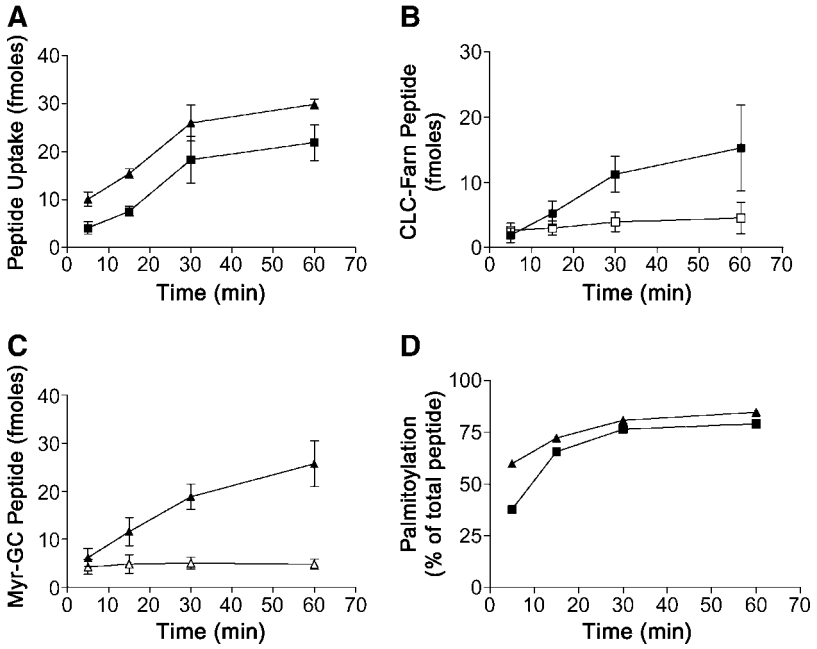

Fig. 5. Time course of peptide palmitoylation by SKOV3 cells. SKOV3 cells were incubated for the indicated times at 37°C with 1 μM NBD-CLC(OMe)-Farn or Myr-GC-NBD peptide. Samples were then extracted and analyzed as described in Materials and Methods. A: The total amount of NBD-CLC(OMe)-Farn (closed squares) or Myr-GC-NBD (closed triangles) peptide accumulation in the cells was determined as the total fluorescence in the samples. B: The amounts of nonpalmitoylated NBD-CLC(OMe)-Farn (open squares) and palmitoylated NBD-CLC(OMe)-Farn (closed squares) are shown. C: The amounts of nonpalmitoylated Myr-GC-NBD (open triangles) and palmitoylated Myr-GC-NBD (closed triangles) are shown. D: The percentages of palmitoylated NBD-CLC(OMe)-Farn (closed squares) and Myr-GC-NBD (closed triangles) peptide are shown. For A–C, values represent means ± SD for triplicate samples in a typical experiment; for D, values represent means ± SEM for three to nine experiments.

only 38% of the NBD-CLC(OMe)-Farn peptide was palmitoylated at the 5 min time point, and the extent of palmitoylation plateaued at ~30 min.

Subcellular trafficking of palmitoylated peptides in SKOV3 cells

To examine the intracellular fate of the lipidated peptides, SKOV3 cells were incubated for 30 min at 37°C with 1 μM NBD-CLC(OMe)-Farn (**Fig. 6A–C**), NBD-ALC(OMe)-Farn (Fig. 6D–F), Myr-GC-NBD (Fig. 6G–I), or Myr-GA-NBD (Fig. 6J–L) peptide and monitored by fluorescence confocal microscopy. At this time point, at least 75% of the NBD-CLC(OMe)-Farn and Myr-GC-NBD peptides are palmitoylated (Fig. 5), whereas none of the NBD-ALC(OMe)-Farn or Myr-GA-NBD peptides are palmitoylated (Fig. 3). Staining with WGA was used to localize the plasma membranes of the cells (Fig. 6A, D, G, J) and produced the expected peripheral staining pattern. Figure 6B, E, H, K indicate that each of the peptides readily entered the cells. Strong peptide fluorescence colocalized with WGA (Fig. 6C, I), indicating that high percentages of the palmitoylated NBD-CLC(OMe)-Farn and Myr-GC-NBD peptides were associated with the plasma membrane. However, minimal peptide fluorescence colocalized with WGA (Fig. 6F, L), indicating that the nonpalmitoylated NBD-ALC(OMe)-Farn and Myr-GA-NBD peptides were not associated with the plasma membrane. In addition, perinuclear peptide fluorescence resembling the Golgi apparatus was observed by all peptides but was much more pronounced with the nonpalmitoylated NBD-ALC(OMe)-Farn and Myr-GA-NBD peptides (Fig. 6E, K) than with the palmitoylated NBD-CLC(OMe)-Farn and Myr-GC-NBD peptides (Fig. 6B, H).

The localization of the peptides to the Golgi apparatus was confirmed by further confocal microscopy studies in which SKOV3 cells were incubated with 1 μM NBD-CLC(OMe)-Farn (**Fig. 7A–C**), NBD-ALC(OMe)-Farn (Fig. 7D–F), Myr-GC-NBD (Fig. 7G–I), or Myr-GA-NBD (Fig. 7J–L) peptide for 30 min at 37°C. The Golgi apparatus was concurrently labeled by the addition of BODIPY TR C_5-ceramide (Fig. 7A, D, G, I). Overlays of the images (Fig. 7C, F, I, L) demonstrated that the bulk of the non-plasma membrane-associated peptide fluorescence of the NBD-CLC(OMe)-Farn and Myr-GC-NBD peptides (Fig. 7C, I) was associated with the Golgi apparatus and that nearly all of the peptide fluorescence of the NBD-ALC(OMe)-Farn and Myr-GA-NBD peptides (Fig. 7F, L) was associated with the Golgi apparatus.

The kinetics of intracellular trafficking of the lipidated peptides were evaluated in studies depicted in **Fig. 8**. SKOV3 cells were incubated with Hoechst for 10 min at 37°C, then with 1 μM NBD-CLC(OMe)-Farn (Fig. 8A–D), NBD-

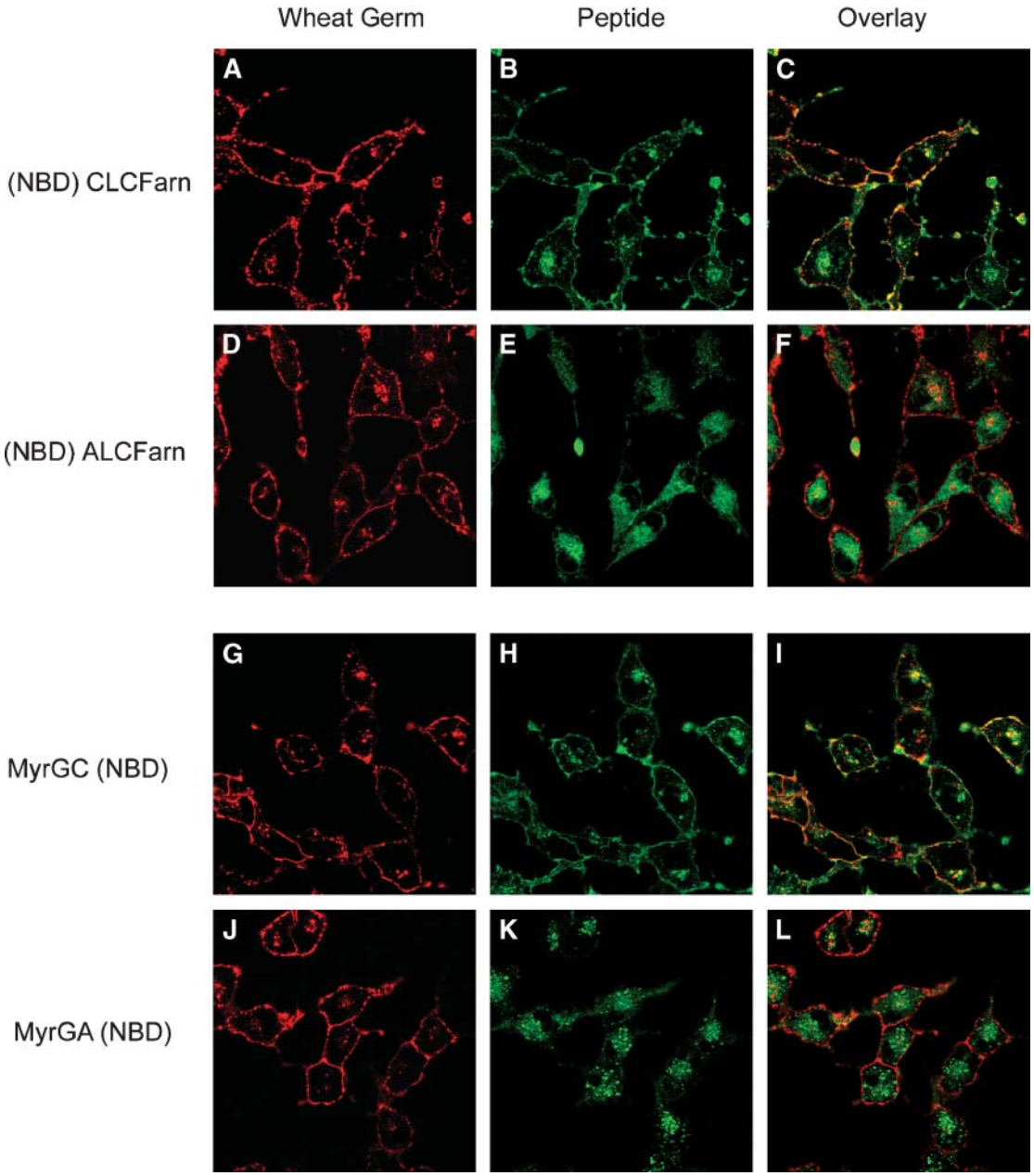

Fig. 6. Localization of lipidated peptides to the plasma membrane. SKOV3 cells were incubated for 30 min at 37°C with 1 μM NBD-CLC(OMe)-Farn (A–C), NBD-ALC(OMe)-Farn (D–F), Myr-GC-NBD (G–I), or Myr-GA-NBD (J–L) peptide. The cells were then quickly washed and imaged by confocal microscopy. The distributions of the NBD-CLC(OMe)-Farn and Myr-GC-NBD fluorescent peptides (which are essentially completely palmitoylated at this time and concentration) are shown in B and H. The distributions of the NBD-ALC(OMe)-Farn and Myr-GA-NBD fluorescent peptides (which are completely nonpalmitoylated) are shown in E and K. Plasma membranes were visualized with AF594-wheat germ agglutinin (A, D, G, J). C, F, I, L show overlays of the two labels in cells exposed to NBD-CLC(OMe)-Farn, NBD-ALC(OMe)-Farn, Myr-GC-NBD, and Myr-GA-NBD peptides, respectively.

ALC(OMe)-Farn (Fig. 8E–H), Myr-GC-NBD (Fig. 8I–L), or Myr-GA-NBD (Fig. 8M–P) peptide at 37°C for 15–120 min. Fifteen minutes was taken as the earliest time point to ensure that the NBD-CLC(OMe)-Farn and Myr-GC-NBD peptides were maximally palmitoylated. Significant amounts of each peptide were observed in the cells at the earliest time point; however, the distribution of NBD-CLC(OMe)-Farn (Fig. 8A) included both the plasma membrane and the Golgi, whereas Myr-GC-NBD (Fig. 8I) was essentially localized exclusively to the plasma membrane. In contrast, at 15 min, both the NBD-ALC(OMe)-Farn (Fig. 8E) and Myr-GA-NBD (Fig. 8M) peptides were localized in the Golgi apparatus. As time progressed, the NBD-CLC(OMe)-Farn peptide (Fig. 8A–D) maintained localization to both the plasma membrane and the Golgi, whereas the Myr-GC-NBD peptide (Fig. 8I–L) increased Golgi localization and became both Golgi- and plasma membrane-associated. In contrast, both the NBD-ALC(OMe)-Farn (Fig. 8E–H) and

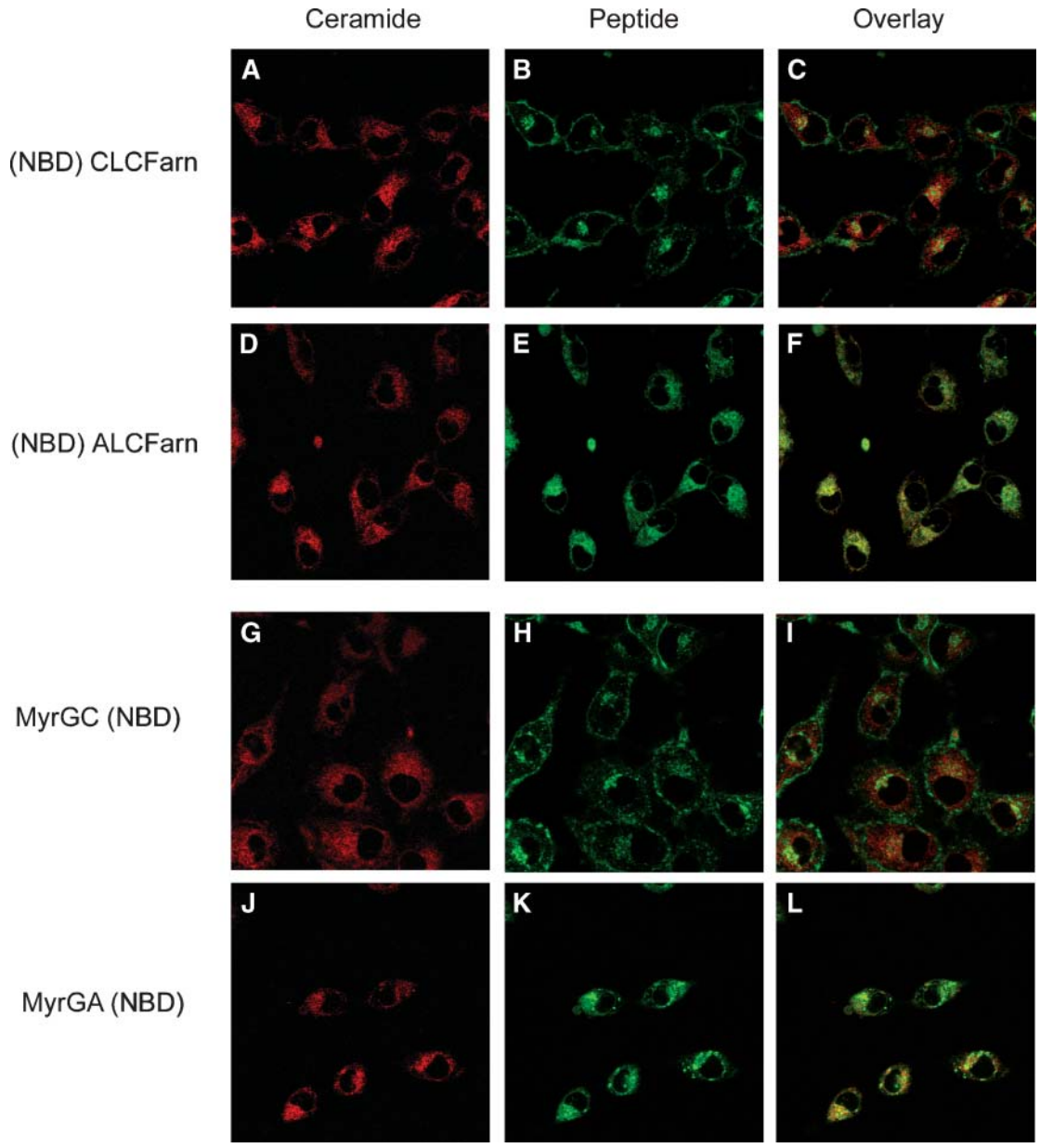

Fig. 7. Trafficking of lipidated peptides to the Golgi apparatus. SKOV3 cells were incubated for 30 min at 37°C with 1 μM NBD-CLC(OMe)-Farn (A–C), NBD-ALC(OMe)-Farn (D–F), Myr-GC-NBD (G–I), or Myr-GA-NBD (J–L) peptide. The cells were then quickly washed and imaged by confocal microscopy. The distributions of the fluorescent peptides are shown in B, E, H, K. The Golgi apparatus was visualized with BODIPY TR C_5-ceramide (A, D, G, J). C, F, I, L show overlays of the two labels in cells exposed to NBD-CLC(OMe)-Farn, NBD-ALC(OMe)-Farn, Myr-GC-NBD, and Myr-GA-NBD peptides, respectively.

Myr-GA-NBD (Fig. 8M–P) peptides remained primarily localized to the Golgi for at least 120 min.

DISCUSSION

The importance of protein lipidation for the proper localization and activity of many signaling proteins has been discussed extensively (2, 7–11, 13–16). Because these proteins are involved in important signaling pathways, including cell survival, proliferation, and activation (28–31), inhibition of their lipidation has been considered an attractive area for new drug development. In this context, most effort has focused on developing inhibitors of farnesyltransferases. Inhibitors of PATs have been slower to develop because the identities of the enzymes are not yet well characterized, although significant progress has occurred over the past few years (27, 41, 42). Seminal studies in yeast identified Efr2/Erf4 as a PAT for yeast Ras (43) and Akr1 as a PAT for yeast casein kinase (44). The conserved DHHC domain of these proteins was hypothesized to represent a signature catalytic motif for PATs and has provided a starting point for the characterization of human PATs. For example, we recently demonstrated that human HIP-14 (DHHC17) is a farnesyl-directed PAT that causes oncogenic transformation of fibroblasts when over-

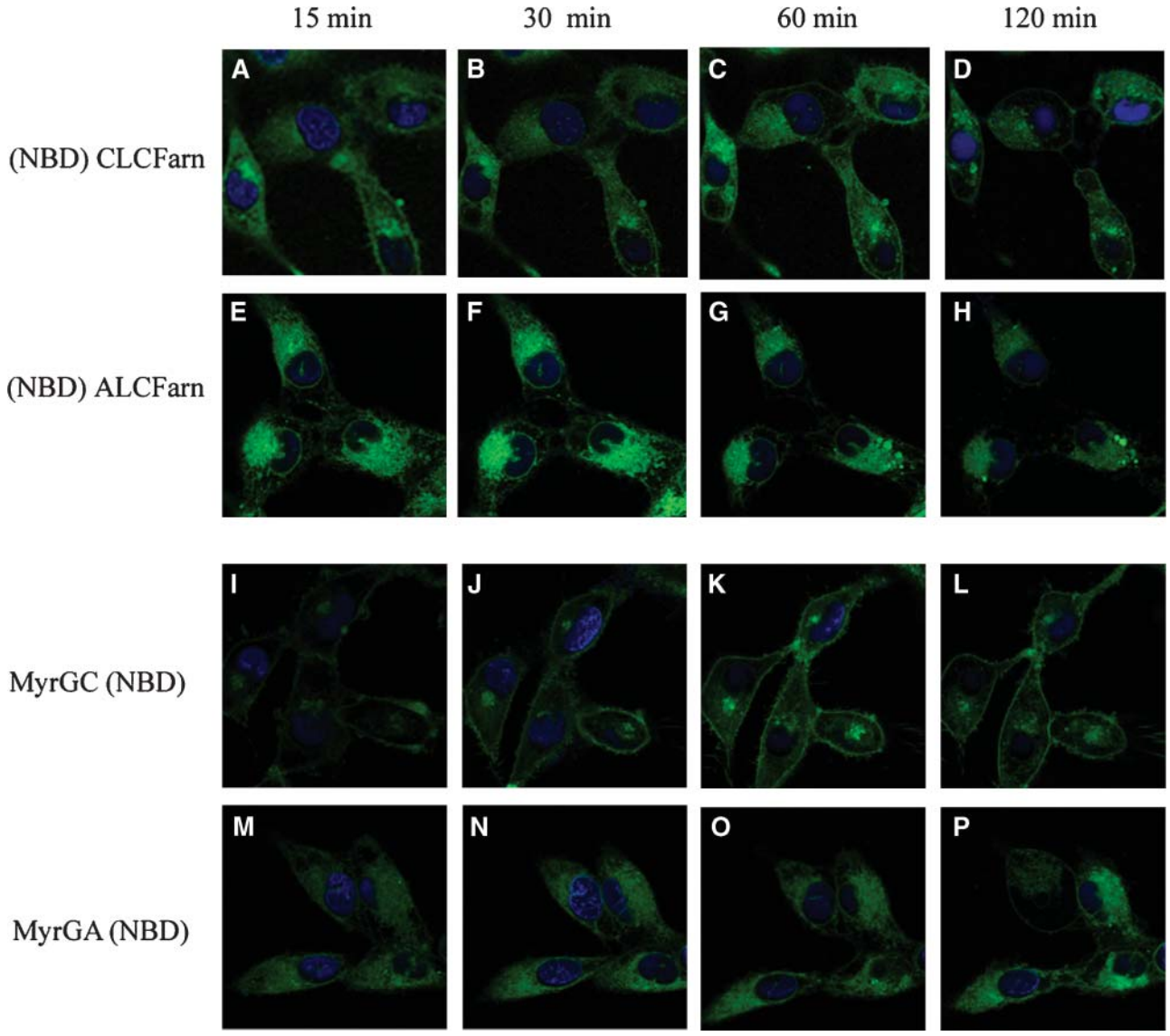

Fig. 8. Time course of lipidated peptide trafficking in SKOV3 cells. SKOV3 cells were incubated for 10 min at 37°C with Hoechst (2 μg/ml) and washed. The cells were subsequently incubated with 1 μM NBD-CLC(OMe)-Farn (A–D), NBD-ALC(OMe)-Farn (E–H), Myr-GC-NBD (I–L), or Myr-GA-NBD (M–P) peptide. The cells were then imaged by confocal microscopy at 15 (A, E, I, M), 30 (B, F, J, N), 60 (C, G, K, O), or 120 (D, H, L, P) min.

expressed (26). Similarly, Swarthout et al. (45) have demonstrated that CGI-89 (DHHC9) palmitoylates N- and H-Ras but not *N*-myristoylated $G\alpha_{i1}$ or GAP-43. However, these studies do not provide definitive identification of the predominant PAT(s) acting within the cellular environment.

Lipidated peptides that mimic palmitoylation motifs have been used by us to quantify palmitoylation in vitro (24–27) and by others to study trafficking, localization, and membrane interactions in live cells (46–50). In particular, studies by Schroeder et al. (46, 47) were instrumental in demonstrating that lipopeptides that mimic protein palmitoylation sites are useful tools for the analyses of PAT activity and protein trafficking. In this study, we sought a quantifiable intact-cell assay to characterize cellular PAT activities using fluorescent peptides that mimic the two putative recognition motifs for enzymatic palmitoylation. We previously used HPLC after in vitro assays to separate fluorescent lipidated PAT substrate peptides from the corresponding products (25–27, 38). The current data clearly demonstrate that the NBD-CLC(OMe)-Farn and Myr-GC-NBD peptides can be palmitoylated by intact SKOV3 cells, whereas the NBD-ALC(OMe)-Farn and Myr-GA-NBD peptides remain nonpalmitoylated. Well-resolved peaks representing the substrate peptides and the palmitoylated products of the Cys-containing peptides were verified by mass spectroscopy and can be quantified by their fluorescence. Therefore, the Cys-containing lipopeptides provide biochemical tools for quantifying both farnesyl- and myristoyl-directed PAT activity within intact cells, and the Ala-containing lipopeptides can serve as nonpalmitoylated controls for localization in confocal analyses.

To further characterize cellular PAT activities, dose-response and time-course studies were performed with each substrate peptide. Dose-response studies indicate that the Myr-GC-NBD peptide accumulates in the cell in a significantly greater amount than the NBD-CLC(OMe)-Farn peptide, which may be attributable to the somewhat smaller size of the Myr-GC-NBD peptide (molecular weight = 738) compared with the NBD-CLC(OMe)-Farn peptide (molecular weight = 920). In addition, data shown in Fig. 4 indicate a difference in the ability of SKOV3 cells to palmitoylate the Myr-GC-NBD and NBD-CLC(OMe)-Farn peptides. Specifically, SKOV3 cells are able to maintain nearly complete palmitoylation of the Myr-GC-NBD peptide regardless of its concentration in the medium. In contrast, the cells could maintain maximal palmitoylation of the NBD-CLC(OMe)-Farn peptide to a concentration of only 1 μM. This suggests that SKOV3 cells have a greater capacity to palmitoylate proteins containing the N-terminal Myr-GC recognition motif than the C-terminal CLC-Farn motif. There are several possible reasons for this, including differences in the abundance and efficiency of the different PAT enzymes as well as differences in thioesterase activity. In any case, the lower cellular capacity of farnesyl-directed PAT activity suggests that this class of PATs may be more amenable to pharmacologic inhibition than the myristoyl-directed PATs.

The time-course studies indicate that the uptake of the Myr-GC-NBD peptide is faster than the uptake of the NBD-CLC(OMe)-Farn peptide and that cellular levels of both peptides plateau after ~30 min. The differences in the kinetics also provide some clues to the location of the different PAT activities. For example, the majority of the Myr-GC-NBD peptide was located at the plasma membrane at 15 and 30 min. Because the palmitoylation of the peptide is essentially complete at those times, the myristoyl-directed PAT activity is most likely located at the plasma membrane. This finding is consistent with previous studies in which the palmitoylation of *N*-myristoylated proteins increased localization to the plasma membrane, especially within lipid rafts (29, 30, 51). Therefore, targeting of these proteins appears to occur through a kinetic trapping process in which the protein is palmitoylated at its final destination. It is less clear, however, where the farnesyl-directed PAT activity is located, because there is a temporal lag before maximal palmitoylation is achieved and a significant amount of the peptide is internalized by 15 min. Therefore, it is unclear whether the NBD-CLC(OMe)-Farn peptide was palmitoylated in the plasma membrane, endoplasmic reticulum, Golgi, or *trans*-Golgi network, all of which have been reported to have PAT activity (52, 53).

As shown previously by others (46, 47), we confirm that the intracellular localizations of the palmitoylated and nonpalmitoylated forms of the farnesyl motif peptides are markedly different. For example, the nonpalmitoylated NBD-ALC(OMe)-Farn peptide localizes exclusively to the Golgi, whereas the palmitoylated NBD-CLC(OMe)-Farn peptide localizes to the Golgi and the plasma membrane. This difference indicates that palmitoylation of the NBD-CLC(OMe)-Farn is required for localization to the plasma membrane and that the lack of palmitoylation confines the peptide to the Golgi. This is similar to the intracellular trafficking of wild-type Ras proteins, in which that Ras localized to intracellular compartments including the endoplasmic reticulum, the Golgi complex, and the plasma membrane (54–58). Additional reports indicate that the farnesyl motif targets Ras to the endoplasmic reticulum and the Golgi complex, whereas palmitoylation is required to exit the Golgi complex (54, 55). Furthermore, the recycling of depalmitoylated and palmitoylated Ras appears to affect the localization of the protein, in that depalmitoylated Ras traffics from the plasma membrane to the Golgi complex, whereas palmitoylated Ras moves from the Golgi complex to the plasma membrane (56, 58). The importance of this cycle to the localization pattern of farnesylated and palmitoylated proteins was further described by Rocks et al. (58), who showed that irreversibly acylated N-Ras is nonspecifically associated with internal membranes, whereas reversibly palmitoylated N-Ras localizes to the Golgi and plasma membrane. Overall, our results support the hypothesis that the PAT responsible for the palmitoylation of Ras is located in the Golgi complex.

The localization of the palmitoylated and nonpalmitoylated myristoyl motif peptides is also different. The nonpalmitoylated Myr-GA-NBD peptide remains localized to the Golgi, whereas the palmitoylated Myr-GC-NBD peptide traffics to the plasma membrane. These results are supported by data from Schroeder et al. (47), who used palmitoylatable Myr-GCG-NBD and nonpalmitoylatable Myr-GSG-NBD peptides in CV-1 cells. They found that the palmitoylatable form of the myristoyl motif peptide was localized primarily to the plasma membrane and that the nonpalmitoylatable form was localized to the Golgi. In addition, *N*-myristoylated and palmitoylated green fluorescent protein chimeras have been found to localize to the Golgi and the plasma membrane (59), which is consistent with the localization of endogenous myristoyl motif-containing proteins such as the Src-related tyrosine kinase Fyn (60). Overall, the localization results obtained in this study indicate that the NBD-CLC(OMe)-Farn and Myr-GCG-NBD peptides mimic the localization patterns of C-terminally farnesylated and palmitoylated proteins and N-terminally myristoylated and palmitoylated proteins, respectively. In each case, the cellular distributions of the palmitoylated and nonpalmitoylated forms of the peptides are markedly different.

In conclusion, we have developed quantitative cell-based model systems to monitor human PAT activities using peptides that mimic the N-terminal myristoyl-palmitoylation and C-terminal farnesyl-palmitoylation motifs. These peptides are cell-permeable and are rapidly palmitoylated by endogenous PATs. These data indicate that SKOV3 human ovarian carcinoma cells have substantially higher myristoyl-directed PAT activity than farnesyl-directed PAT activity, suggesting that the palmitoylation of Ras and other farnesyl motif proteins could be inhibited selectively. In related studies, we recently described the identification and characterization of selective inhibitors of farnesyl-directed and myristoyl-directed PATs that may

provide new therapeutic agents (27). The present model systems also provide means to identify additional human PATs (e.g., using gene-specific small interfering RNA knockdown of potential targets).

The authors acknowledge the assistance of Dr. Charles E. Ducker in the development of the HPLC protocols. The authors also thank the staff at the Confocal Microscopy Core and the NMR Core at the Medical University of South Carolina for the use of instrumentation for these studies. Financial support was provided by National Institutes of Health Grant 2 R01 CA-75248 (C.D.S.).

REFERENCES

1. Dunphy, J. T., and M. E. Linder. 1998. Signalling functions of protein palmitoylation. *Biochim. Biophys. Acta.* **1436:** 245–261.
2. Milligan, G., M. Parenti, and A. I. Magee. 1995. The dynamic role of palmitoylation in signal transduction. *Trends Biochem. Sci.* **20:** 181–187.
3. Resh, M. D. 1999. Fatty acylation of proteins: new insights into membrane targeting of myristoylated and palmitoylated proteins. *Biochim. Biophys. Acta.* **1451:** 1–16.
4. Linder, M. E., and R. J. Deschenes. 2007. Palmitoylation: policing protein stability and traffic. *Nat. Rev. Mol. Cell Biol.* **8:** 74–84.
5. Greaves, J., and L. H. Chamberlain. 2007. Palmitoylation-dependent protein sorting. *J. Cell Biol.* **176:** 249–254.
6. Resh, M. D. 2006. Palmitoylation of ligands, receptors, and intracellular signaling molecules. *Sci. STKE.* **2006:** re14.
7. Mumby, S. M. 1997. Reversible palmitoylation of signaling proteins. *Curr. Opin. Cell Biol.* **9:** 148–154.
8. Dudler, T., and M. H. Gelb. 1996. Palmitoylation of Ha-Ras facilitates membrane binding, activation of downstream effectors, and meiotic maturation in Xenopus oocytes. *J. Biol. Chem.* **271:** 11541–11547.
9. Everson, W. V., and E. J. Smart. 2001. Influence of caveolin, cholesterol, and lipoproteins on nitric oxide synthase: implications for vascular disease. *Trends Cardiovasc. Med.* **11:** 246–250.
10. Hurley, J. H., A. L. Cahill, K. P. Currie, and A. P. Fox. 2000. The role of dynamic palmitoylation in Ca^{2+} channel inactivation. *Proc. Natl. Acad. Sci. USA.* **97:** 9293–9298.
11. Milligan, G., M. A. Grassie, A. Wise, D. J. MacEwan, A. I. Magee, and M. Parenti. 1995. G-protein palmitoylation: regulation and functional significance. *Biochem. Soc. Trans.* **23:** 583–587.
12. Tanimura, N., S. I. Saitoh, S. Kawano, A. Kosugi, and K. Miyake. 2006. Palmitoylation of LAT contributes to its subcellular localization and stability. *Biochem. Biophys. Res. Commun.* **341:** 1177–1183.
13. Hancock, J. F., H. Paterson, and C. J. Marshall. 1990. A polybasic domain or palmitoylation is required in addition to the CAAX motif to localize p21ras to the plasma membrane. *Cell.* **63:** 133–139.
14. Zhang, W., J. Sloan-Lancaster, J. Kitchen, R. P. Trible, and L. E. Samelson. 1998. LAT: the ZAP-70 tyrosine kinase substrate that links T cell receptor to cellular activation. *Cell.* **92:** 83–92.
15. Honda, Z., T. Suzuki, H. Kono, M. Okada, T. Yamamoto, C. Ra, Y. Morita, and K. Yamamoto. 2000. Sequential requirements of the N-terminal palmitoylation site and SH2 domain of Src family kinases in the initiation and progression of FcepsilonRI signaling. *Mol. Cell. Biol.* **20:** 1759–1771.
16. Kosugi, A., F. Hayashi, D. R. Liddicoat, K. Yasuda, S. Saitoh, and T. Hamaoka. 2001. A pivotal role of cysteine 3 of Lck tyrosine kinase for localization to glycolipid-enriched microdomains and T cell activation. *Immunol. Lett.* **76:** 133–138.
17. Gelb, M. H., L. Brunsveld, C. A. Hrycyna, S. Michaelis, F. Tamanoi, W. C. Van Voorhis, and H. Waldmann. 2006. Therapeutic intervention based on protein prenylation and associated modifications. *Nat Chem Biol.* **2:** 518–528.
18. Resh, M. D. 1996. Regulation of cellular signalling by fatty acid acylation and prenylation of signal transduction proteins. *Cell. Signal.* **8:** 403–412.
19. Hancock, J. F., A. I. Magee, J. E. Childs, and C. J. Marshall. 1989. All ras proteins are polyisoprenylated but only some are palmitoylated. *Cell.* **57:** 1167–1177.
20. Eungdamrong, N. J., and R. Iyengar. 2007. Compartment-specific feedback loop and regulated trafficking can result in sustained activation of Ras at the Golgi. *Biophys. J.* **92:** 808–815.
21. Pechlivanis, M., and J. Kuhlmann. 2006. Hydrophobic modifications of Ras proteins by isoprenoid groups and fatty acids. More than just membrane anchoring. *Biochim. Biophys. Acta.* **1764:** 1914–1931.
22. Degtyarev, M. Y., A. M. Spiegel, and T. L. Jones. 1994. Palmitoylation of a G protein alpha i subunit requires membrane localization not myristoylation. *J. Biol. Chem.* **269:** 30898–30903.
23. Morales, J., C. S. Fishburn, P. T. Wilson, and H. R. Bourne. 1998. Plasma membrane localization of G alpha z requires two signals. *Mol. Biol. Cell.* **9:** 1–14.
24. Varner, A. S., M. L. De Vos, S. P. Creaser, B. R. Peterson, and C. D. Smith. 2002. A fluorescence-based high performance liquid chromatographic method for the characterization of palmitoyl acyl transferase activity. *Anal. Biochem.* **308:** 160–167.
25. Varner, A. S., C. E. Ducker, Z. Xia, Y. Zhuang, M. L. De Vos, and C. D. Smith. 2003. Characterization of human palmitoyl-acyl transferase activity using peptides that mimic distinct palmitoylation motifs. *Biochem. J.* **373:** 91–99.
26. Ducker, C. E., E. M. Stettler, K. J. French, J. J. Upson, and C. D. Smith. 2004. Huntingtin interacting protein 14 is an oncogenic human protein: palmitoyl acyltransferase. *Oncogene.* **23:** 9230–9237.
27. Ducker, C. E., L. K. Griffel, R. A. Smith, S. N. Keller, Y. Zhuang, Z. Xia, J. D. Diller, and C. D. Smith. 2006. Discovery and characterization of inhibitors of human palmitoyl acyltransferases. *Mol. Cancer Ther.* **5:** 1647–1659.
28. Downward, J. 2003. Targeting RAS signalling pathways in cancer therapy. *Nat. Rev. Cancer.* **3:** 11–22.
29. Shenoy-Scaria, A. M., D. J. Dietzen, J. Kwong, D. C. Link, and D. M. Lublin. 1994. Cysteine3 of Src family protein tyrosine kinase determines palmitoylation and localization in caveolae. *J. Cell Biol.* **126:** 353–363.
30. Rodgers, W., B. Crise, and J. K. Rose. 1994. Signals determining protein tyrosine kinase and glycosyl-phosphatidylinositol-anchored protein targeting to a glycolipid-enriched membrane fraction. *Mol. Cell. Biol.* **14:** 5384–5391.
31. Finco, T. S., T. Kadlecek, W. Zhang, L. E. Samelson, and A. Weiss. 1998. LAT is required for TCR-mediated activation of PLCgamma1 and the Ras pathway. *Immunity.* **9:** 617–626.
32. Leonard, D. M. 1997. Ras farnesyltransferase: a new therapeutic target. *J. Med. Chem.* **40:** 2971–2990.
33. Waddick, K. G., and F. M. Uckun. 1998. Innovative treatment programs against cancer. I. Ras oncoprotein as a molecular target. *Biochem. Pharmacol.* **56:** 1411–1426.
34. Pompliano, D. L., E. Rands, M. D. Schaber, S. D. Mosser, N. J. Anthony, and J. B. Gibbs. 1992. Steady-state kinetic mechanism of Ras farnesyl:protein transferase. *Biochemistry.* **31:** 3800–3807.
35. Chen, W. J., D. A. Andres, J. L. Goldstein, D. W. Russell, and M. S. Brown. 1991. cDNA cloning and expression of the peptide-binding beta subunit of rat p21ras farnesyltransferase, the counterpart of yeast DPR1/RAM1. *Cell.* **66:** 327–334.
36. Kohl, N. E., S. D. Mosser, S. J. deSolms, E. A. Giuliani, D. L. Pompliano, S. L. Graham, R. L. Smith, E. M. Scolnick, A. Oliff, and J. B. Gibbs. 1993. Selective inhibition of ras-dependent transformation by a farnesyltransferase inhibitor. *Science.* **260:** 1934–1937.
37. James, G. L., J. L. Goldstein, M. S. Brown, T. E. Rawson, T. C. Somers, R. S. McDowell, C. W. Crowley, B. K. Lucas, A. D. Levinson, and J. C. Marsters, Jr. 1993. Benzodiazepine peptidomimetics: potent inhibitors of Ras farnesylation in animal cells. *Science.* **260:** 1937–1942.
38. Varner, A., M. De Vos, S. Creaser, B. Peterson, and C. Smith. 2002. A fluorescence-based high performance liquid chromatographic method for the characterization of palmitoyl acyl transferase activity. *Anal. Biochem.* **308:** 160–167.
39. Xia, Z., and C. D. Smith. 2001. Efficient synthesis of a fluorescent farnesylated Ras peptide. *J. Org. Chem.* **66:** 5241–5244.
40. Pagano, R. E., O. C. Martin, H. C. Kang, and R. P. Haugland. 1991. A novel fluorescent ceramide analogue for studying membrane traffic in animal cells: accumulation at the Golgi apparatus results in altered spectral properties of the sphingolipid precursor. *J. Cell Biol.* **113:** 1267–1279.
41. Linder, M. E., and R. J. Deschenes. 2004. Model organisms lead the way to protein palmitoyltransferases. *J. Cell Sci.* **117:** 521–526.
42. Mitchell, D. A., A. Vasudevan, M. E. Linder, and R. J. Deschenes.

2006. Protein palmitoylation by a family of DHHC protein S-acyltransferases. *J. Lipid Res.* **47:** 1118–1127.
43. Lobo, S., W. K. Greentree, M. E. Linder, and R. J. Deschenes. 2002. Identification of a Ras palmitoyltransferase in *Saccharomyces cerevisiae*. *J. Biol. Chem.* **277:** 41268–41273.
44. Roth, A. F., Y. Feng, L. Chen, and N. G. Davis. 2002. The yeast DHHC cysteine-rich domain protein Akr1p is a palmitoyl transferase. *J. Cell Biol.* **159:** 23–28.
45. Swarthout, J. T., S. Lobo, L. Farh, M. R. Croke, W. K. Greentree, R. J. Deschenes, and M. E. Linder. 2005. DHHC9 and GCP16 constitute a human protein fatty acyltransferase with specificity for H- and N-Ras. *J. Biol. Chem.* **280:** 31141–31148.
46. Schroeder, H., R. Leventis, S. Rex, M. Schelhaas, E. Nagele, H. Waldmann, and J. R. Silvius. 1997. S-Acylation and plasma membrane targeting of the farnesylated carboxyl-terminal peptide of N-ras in mammalian fibroblasts. *Biochemistry.* **36:** 13102–13109.
47. Schroeder, H., R. Leventis, S. Shahinian, P. A. Walton, and J. R. Silvius. 1996. Lipid-modified, cysteinyl-containing peptides of diverse structures are efficiently S-acylated at the plasma membrane of mammalian cells. *J. Cell Biol.* **134:** 647–660.
48. Creaser, S. P., and B. R. Peterson. 2002. Sensitive and rapid analysis of protein palmitoylation with a synthetic cell-permeable mimic of SRC oncoproteins. *J. Am. Chem. Soc.* **124:** 2444–2445.
49. Peters, C., M. Wagner, M. Volkert, and H. Waldmann. 2002. Bridging the gap between cell biology and organic chemistry: chemical synthesis and biological application of lipidated peptides and proteins. *Naturwissenschaften.* **89:** 381–390.
50. Silvius, J. R. 2002. Lipidated peptides as tools for understanding the membrane interactions of lipid-modified proteins. *In* Current Topics in Membranes. Vol. 52. S. Simon, editor. Academic Press, New York. 371–395.
51. Hawash, I. Y., X. E. Hu, A. Adal, J. M. Cassady, R. L. Geahlen, and M. L. Harrison. 2002. The oxygen-substituted palmitic acid analogue, 13-oxypalmitic acid, inhibits Lck localization to lipid rafts and T cell signaling. *Biochim. Biophys. Acta.* **1589:** 140–150.
52. Dunphy, J. T., W. K. Greentree, C. L. Manahan, and M. E. Linder. 1996. G-protein palmitoyltransferase activity is enriched in plasma membranes. *J. Biol. Chem.* **271:** 7154–7159.
53. Liu, L., T. Dudler, and M. H. Gelb. 1996. Purification of a protein palmitoyltransferase that acts on H-Ras protein and on a C-terminal N-Ras peptide. *J. Biol. Chem.* **271:** 23269–23276.
54. Apolloni, A., I. A. Prior, M. Lindsay, R. G. Parton, and J. F. Hancock. 2000. H-ras but not K-ras traffics to the plasma membrane through the exocytic pathway. *Mol. Cell. Biol.* **20:** 2475–2487.
55. Choy, E., V. K. Chiu, J. Silletti, M. Feoktistov, T. Morimoto, D. Michaelson, I. E. Ivanov, and M. R. Philips. 1999. Endomembrane trafficking of ras: the CAAX motif targets proteins to the ER and Golgi. *Cell.* **98:** 69–80.
56. Goodwin, J. S., K. R. Drake, C. Rogers, L. Wright, J. Lippincott-Schwartz, M. R. Philips, and A. K. Kenworthy. 2005. Depalmitoylated Ras traffics to and from the Golgi complex via a nonvesicular pathway. *J. Cell Biol.* **170:** 261–272.
57. Gomez, G. A., and J. L. Daniotti. 2005. H-Ras dynamically interacts with recycling endosomes in CHO-K1 cells: involvement of Rab5 and Rab11 in the trafficking of H-Ras to this pericentriolar endocytic compartment. *J. Biol. Chem.* **280:** 34997–35010.
58. Rocks, O., A. Peyker, M. Kahms, P. J. Verveer, C. Koerner, M. Lumbierres, J. Kuhlmann, H. Waldmann, A. Wittinghofer, and P. I. Bastiaens. 2005. An acylation cycle regulates localization and activity of palmitoylated Ras isoforms. *Science.* **307:** 1746–1752.
59. McCabe, J. B., and L. G. Berthiaume. 1999. Functional roles for fatty acylated amino-terminal domains in subcellular localization. *Mol. Biol. Cell.* **10:** 3771–3786.
60. Wolven, A., H. Okamura, Y. Rosenblatt, and M. D. Resh. 1997. Palmitoylation of p59fyn is reversible and sufficient for plasma membrane association. *Mol. Biol. Cell.* **8:** 1159–1173.